Master Lab: Diamonds for Sensing Applications

D. Palani, A. Das, J.-P. Schröder, O. Orlov, and U. Warring
Albert-Ludwigs-Universität Freiburg, Physikalisches Institut,
Hermann-Herder-Straße 3, 79104 Freiburg, Germany
(Dated: November 8, 2021)

Diamonds inhabit a variety of color centres, one of particular interest is the so-called nitrogen-vacancy (NV) centre. It is studied in great detail in quantum physics research and it is a promising platform for sensing applications on a molecular level. The goals of this lab course is for the students to investigate the principles of magnetic field sensing with NV centres in diamonds. During the course they learn to apply/optimise laser light and microwave fields in the context of quantum physics experiments and to analyse spectral resonances.

Keywords: Nano-diamonds, diamond lattice, NV centre, diode laser, microwaves, fluorescence spectroscopy, optically detected magnetic resonance, and Zeeman effect

Training skills: Optics and laser beam alignment, electronics, and data acquisition/analysis.

CONTENTS

I. INTRODUCTION

Diamonds sparkle in a variety of colours and attract our attention for many different reasons. Besides their appeal as gemstones, they are known for their outstanding mechanical hardness, heat conductivity, electrical resistivity, chemical stability, and optical transparency. The natural occurrence in more than one distinct colour originates from so-called colour centres in diamonds. They are identified as fluorescent lattice defects, where carbon atoms are replaced by impurity atoms or vacant lattice sites. Each kind of defect is uniquely identifiable by its fluorescent/absorption spectrum. Today, we know more than several hundred distinct colour centres [1]. The physical properties of such defects in synthetic diamonds are studied, as they rise the promise for several different novel application within the fields of physics, nanotechnology, and life science [2–7]. For the latter, it is crucial that diamonds are judged non-toxic and, as such, they are well suited for bio-medical applications. They are heavily investigated in the context of, e.g., drug delivery and bio imaging [3]. A particular defect in diamonds has caught the attention of scientists during the last decades. It is comprised by a nitrogen atom and a neighbouring, vacant lattice site; the so-called nitrogen vacancy (NV) centre [5, 8]. In physics, its quantum mechanical properties are studied in detail, as those can be used for quantum information [2], simulation [6], and metrology [7] applications.

Notably, some of the employed methods and techniques for quantum control of the NV centres were developed in the field of nuclear magnetic resonance and atomic physics during the last century. These methodologies, e.g., enable high-precision measurements and control of the quantum degrees of freedom of individual atoms and are commonly applied for most accurate and precise atomic clocks and quantum information processing [9]. Unfortunately, quantum experiments require highest efforts in isolating individual, single atoms from their environment [10]. For example, ultra-high vacuum conditions and temperatures close to the absolute zero are essential and make versatile applications of atoms as sensors challenging. As the quantum nature (coherence) of NV centres is well protected by the surrounding diamond lattice, its sensor properties can be harnessed even under ambient conditions. NV centres are, therefore, ideal for sensing in rough environments, e.g., in aqueous solutions for life science applications. They have been demonstrated to be sensitive, e.g., to magnetic [11–13] and electric [14] fields, temperature [15], and pressure [16]. To use these defects as sensors, they are packed in small diamond crystallites of a few tens of nanometers in diameter [3, 5, 7] with about 10^9 carbon atoms. Recently, it has been demonstrated in a proof-of-principle experiment that quantum measurements on nano-diamonds can be performed even inside living cells [17]. However, to harness the full potential of such nanoscale sensors for metrology applications suitable techniques are required to control their spatial position and orientation, as well as, to efficiently manipulate their quantum state. Currently, several techniques are being investigated for spatial control [18–21], including optical tweezers and scanning probe approaches, in which nano-diamonds are attached, e.g., to atomic force microscope tips. In one of our lines of research, we investigate a novel approach to achieve that: We employ control and sensing methodologies that we previously demonstrated with individually trapped atomic ions and commonly use in the group of Prof. Schätz.

In this lab course, we study the spectral characteristics of NV centres in micro-sized diamonds. This includes measurements of their fluorescence spectra [5, 7] to identify different NV centres and recordings of optically detected magnetic resonances [5, 7] in the microwave regime. Finally, magnetic field sensing possibilities are investigated and we may reconstruct the orientation of the mono crystalline lattice within the laboratory coordinate system. In combination we learn the prerequisites for quantum state control of single NV centres for sensing applications.

Note, our instruction outlines theoretical and experimental aspects, introduces relevant keywords (see in each section), and presents relevant literature. For proper preparation for the lab work, you may need to study additional textbooks or other sources depending on your specific knowledge level. In particular, the Master thesis of Deviprasath Palani introduces relevant details of our setup [22]. Details of experimental procedures are discussed and elaborated together with the teaching assistant during the lab class.

A. NV centres within the lattice structure

A nitrogen vacancy centre in the diamond lattice is comprised by a nitrogen atom replacing a carbon atom and an adjacent vacant lattice site. The spatial characteristics of the centre, i.e., it's symmetries and other environmental conditions, tune the associated electronic state configurations, cp. Sec. I B. The density of NV centres within (natural and synthetic) diamonds strongly depends on the conditions under which they are formed [5] and can even vary within individual diamonds that have been produced under the same conditions. Most efficiently, these centres are introduced in type-1b synthetic diamond samples through electron irradiation with energies of approx. 2 MeV and annealing at 600 K under vacuum conditions [5]. In this lab course we are using commercial mono crystalline powders (MSYmicron-diamond powder from Microdiamant AG) with different sized diamonds in the range of 25 nm

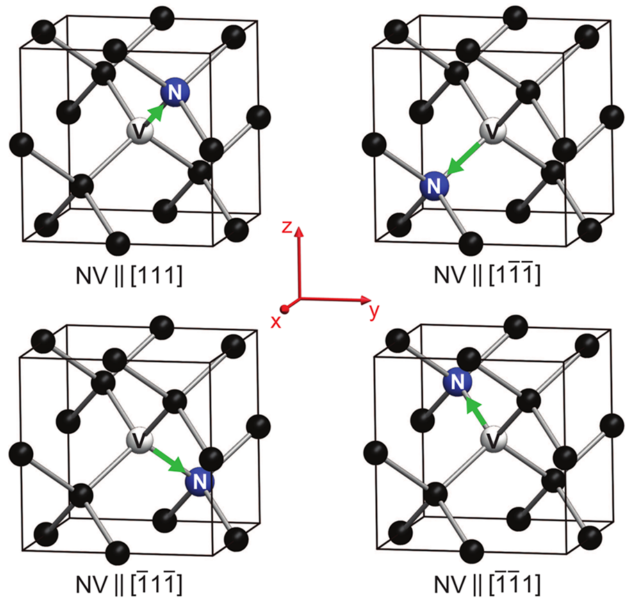

FIG. 1. Orientation of the NV centres within the diamond lattice. Four different orientations are depicted within the face-centred cubic Bravais lattice and their orientations are described according to Miller indices. In addition, there are four orientations (not shown), where the nitrogen atom and the vacancy change places. Figure adapted from Ref. [23]

up to 25 μm. In these samples the NV density has not been intentionally increased during formation as they are typically used for diamond tools. In general, the symmetry axis of the NV centres can (only) be aligned along the crystallographic directions and Fig. 1 depicts possible orientations with the face-centred cubic Bravais lattice. Typically, the eight possible orientations are labelled according to corresponding Miller indices.

Keywords: NV centres ($NV^{-,0,+}$), diamond lattice structure, symmetry axis, fcc Bravais lattice, Miller indices, crystal defects, and mono crystalline structure.

Prep. question example: What are possible spatial orientations of centres within the diamond lattice? How are they specified?

B. Quantum properties of NV centres and sensing applications

Over the past decades, research studying NV centres has provided us with an understanding of the underlying physics, based on empirical as well as ab initio results [5, 7]. Today, we can understand the properties of their magnetic moment, that are judged most important for future applications, in a simplified energy-level diagram, illustrated in Fig. 2. Note, here and in the following, we restrict ourselves to the negatively charged NV

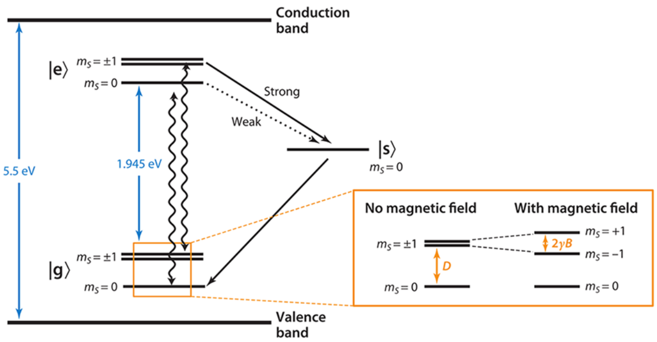

FIG. 2. Simplified energy level diagram of NV^- (not to scale). The electronic ground and excited, triplet states are labelled $|g\rangle$ and $|e\rangle$, respectively, while an effective, singlet state is marked $|s\rangle$; sub levels are labelled according to their spin quantum numbers m_s. Dipole allowed transitions are illustrated with wiggly arrows and other decay channels via are shown with straight arrows. Inset illustrates the Zeeman effect of the ground state manifold that allows for magnetic field sensing. The ground state manifold can be controlled using microwave radiation at around $D \simeq 2\pi \times 2870\,\mathrm{MHz}$. Figure adapted from Ref. [7]

centres [5, 7]. The figure shows three electronic levels, two triplets and one singlet state. The ground state, $|g\rangle$,has a symmetry of ${}^3\mathrm{A}_2$, the excited state, $|e\rangle$, has a symmetry of ${}^3\mathrm{E}$, while the intermediate, metastable state, $|s\rangle$, actually involves two states with symmetries ${}^1\mathrm{A}_1$ and ${}^1\mathrm{E}$. The so-called zero phonon line (ZPL), the main optical transition with a lifetime of about 10 to 30 ns [5], couples $|g\rangle$ with $|e\rangle$ and has a wavelength of $\lambda_{\mathrm{ZPL}} \simeq 637\,\mathrm{nm}$. Typically it is excited with $\lambda_{\mathrm{exc}} \simeq 532\,\mathrm{nm}$, while it can be excited in a broad band below. However, the fluorescence ranges also over a broad range and only a few percent of the photons are emitted into the ZPL; the major part emits into vibrational sidebands in the range of 630 to 800 nm [5, 7]. Non-radiative decay to $|s\rangle$ can also occur, which, in turn, has a lifetime of about 250 ns. The fraction of radiative decay from $|e\rangle$ depends on the spin state, as illustrated in Fig. 2 and this leads to a temporary optical contrast of about 30% between the states $|g, m_{\mathrm{s}} = 0\rangle$ (bright state) and $|g, m_{\mathrm{s}} = \pm 1\rangle$ (dark state) when probing with the excitation light; this effect can be used for state detection/discrimination. After many scattering events the decay via $|s\rangle$ pumps population into $|g, m_{\mathrm{s}} = 0\rangle$ and this can be used as state preparation. Ground-state manipulation can be achieved by microwave radiation near $\omega_{\mathrm{mw}} = 2\pi \times 2870\,\mathrm{MHz}$ (for zero external magnetic field, $B \simeq 0$) coupling $|g, m_{\mathrm{s}} = 0\rangle$ and $|g, m_{\mathrm{s}} = \pm 1\rangle$. For $B > 0$, the two (near) degenerate states $|g, m_{\mathrm{s}} = +1\rangle$ and $|g, m_{\mathrm{s}} = -1\rangle$ split according to the Zeeman effect $\Delta E_{\mathrm{Zeeman}} = \mu_{\mathrm{B}}\, g_{\mathrm{s}}\, m_{\mathrm{s}}\, B$, where $g_{\mathrm{s}} \simeq 2$ denotes the Lande factor of the electron spin and μ_{B} the Bohr magneton. Typical experimental setups [5, 7] include a confocal microscope for application of excitation light and detection of fluorescence light. Further, the experimental setup includes a microwave sender, commonly, connected to a transmission line (coplanar waveguide) that is brought into close proximity to the NV centre. For some experiments, it suffices to hold nanodiamonds on a glass slide under ambient conditions. The most effective sensing protocols would employ pulsed sequences, where an initial pulse of the excitation light prepares the bright state, followed by customised state manipulation pulses of microwave radiation, and concluded with a short pulse of the excitation light for state detection. Those customised state manipulation pulses are typically inspired by original work on nuclear magnetic resonance and atomic clocks [9]. For typical experiments on NV centres, the total protocol duration is limited by decoherence effects of the ground state manifold. At room temperature the dominating effect is spin-lattice relaxation, which happens on a time scale of a few milliseconds [5, 7]. Using such pulsed sequences, it has been demonstrated that NV centres can detect static magnetic fields [11–13] with a sensitivity of better than $0.36\,\mu\mathrm{T}/\sqrt{\mathrm{Hz}}$ based on the above discussed Zeeman effect. Moreover, employing other effects that tune the details of the spin properties, it has been shown, e.g., to detect static electric fields [14] with a sensitivity of $5.8\,\mathrm{kV/cm}/\sqrt{\mathrm{Hz}}$, temperature [15] with $0.1\,\mathrm{K}/\sqrt{\mathrm{Hz}}$, and pressure [16] with $0.6\,\mathrm{MPa}/\sqrt{\mathrm{Hz}}$ with single NV centres.

Keywords: energy-level diagram, quantum numbers, degenerate energy levels, optical transition, fluorescence, lifetime, (meta)stable states, magnetic moment, spin, singlet and triplet state, vibrational sidebands, (non-)radiative decay, zero phonon line, Zeeman effect/splitting, confocal microscope, and (de-)coherence.

Prep. question example: Sketch a simplified energy level diagram, label important transitions and discuss relevant sensing properties. What is the basis for magnetic field sensing? Give and discuss the appropriate formula.

C. NV fluorescence and optically detected magnetic resonances

In this lab course, we are using continues measurement sequences that are sufficient for our purposes and require less complex data acquisition systems. But, they are less sensitive since they do not rely on coherence effects. In order to identify diamonds with negative NV centres, first of all we need to pick diamonds that emit red light when continuously excited with green laser light. In Figure 3, we show an example of a fluorescence spectrum recorded with our lab course setup. Here, we find a ZPL at about 640 nm that identifies the presence of negative centres.

In addition, we can optically detect magnetic resonances of such centres. Again, we continuously apply laser excitation, but combined with microwave radiation at about $2\pi \times 2.85\,\mathrm{GHz}$, and record the fluorescence with a photo detector. In this way we can monitor variable magnetic fields. Typical results of two of such measurements are shown in Fig. 4. Data is depicted in

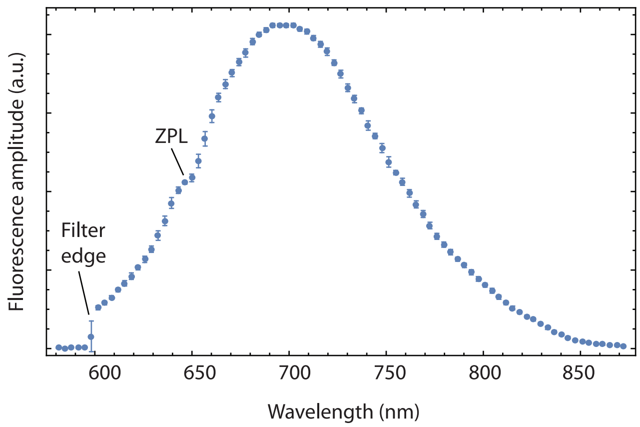

FIG. 3. Fluorescence spectrum of NV centres in micro-sized diamonds at room temperature. Laser light at 519 nm continuously excites fluorescence of the centres in the diamond. The spectrum is dominated by the vibrational band of the lattice. The zero phonon line (ZPL) at $\simeq 640\,\mathrm{nm}$ of the negative NV centres is indicated. The sharp edge at $\simeq 600\,\mathrm{nm}$, results from an optical high-pass filter that is used to reduce scattered light from the excitation laser.

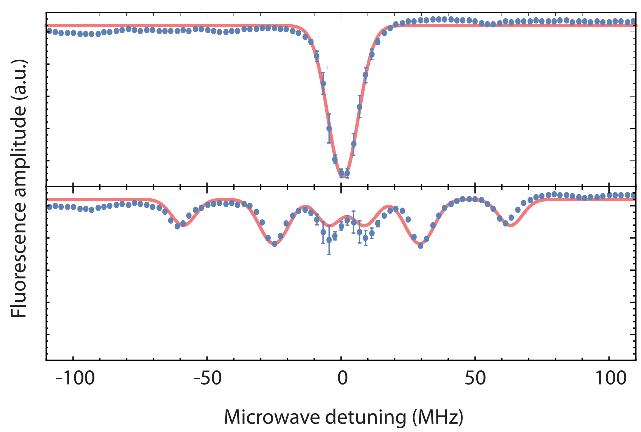

FIG. 4. Optically detected magnetic resonances for variable external magnetic field. Data points are the result of an average of 64 repetitions and solid lines depict model fits to the data. (Top) Microwave spectrum for an external magnetic field strength of $B \simeq 0$ (only stray magnetic fields are present). (Bottom) Spectrum for $B \simeq 25\,\mathrm{G}$, the orientation of the diamond lattice with respect to the external magnetic field axis can be estimated from the observed Zeeman splitting and due to the fact that multiple NV centres are observed simultaneously.

comparison to a corresponding model fit (solid lines). The top graph depicts a single resonance for an external magnetic field close to zero, while the bottom illustrates multiple resonances at an field strength of $B \simeq 23\,\mathrm{G}$. More than two lines are the result of multiple defects that are aligned in multiple directions, i.e., in the studied micro diamond we find more than one NV centre. From the line splittings, we can determine the lattice orientation of a mono crystalline diamond with respect to the direction of the external field. However, this estimation may require to subsequently record spectra with magnetic fields from various directions.

Keywords: fluorescence spectroscopy, optically detected magnetic resonance (ODMR), and optical contrast.

Prep. question example: Explain the processes that lead to a signal in the ODMR spectrum and highlight the interplay of the optical and microwave fields.

II. EXPERIMENTAL SETUP

During the lab course, students work with an experimental setup that they are required to characterise and optimise, cp Sec. III B for details. In the following, we give a brief overview of the available equipment and a description of one possible realisation of such a final setup used for the investigation of NVs in diamonds, see Sec. II C. For their studies, students need to employ various optical, microwave, and other electronic components. In particular, calibration setups require individual rearrangements of the components and students are free to combine available equipment. For a list of the most important elements, we refer to Sec. IV

A. Laser source and optical components

As a light source, we utilise a diode laser with a maximum output power of 100 mW and a wavelength of about 519 nm. This source is classified as a Class-3b system, and it is required that users wear appropriate laser safety goggles when operating the laser. The turnkey system can be controlled via a software interface and is fibre coupled. A tune able fibre coupler is used to optimise the spatial characteristics of the laser beam and several additional optical elements, e.g., aspheric lenses, beam splitters, dichroic mirrors, and filters, are available for the experiments. In addition, we deploy a compact CMOS camera to spatial resolve individual micro-sized diamonds. To study characteristics of the fluorescence light of NV centres in these diamond samples, we install a compact spectrometer and an avalanche photo diode (APD).

Keywords: diode laser, photo diode, avalanche photo diode (APD), fibre coupler, dichroic mirror, optical (long/band-pass) filters, beam splitter, (aspheric) lens, optical spectrometer, and power meter.

B. Electronic and microwave equipment

For the measurements of the optically detected magnetic resonances, of the ground-state manifold we

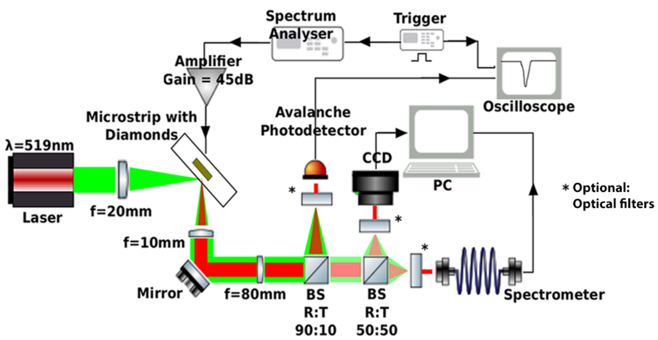

FIG. 5. Schematic of the overall experimental setup (not to scale). Micro sized diamonds are placed on a micro-strip line that is used as a transmission line for microwave currents. The microwave source (output of a spectrum analyser) is amplified and fed into the coplanar waveguide via SMA connectors. Laser light at about 519 nm and up to 100 mW (Class-3b laser system; laser safety goggles need to be worn whenever the laser is operated) excites fluorescence of NV centres. An imaging setup guides green stray light and red fluorescence light to the detection region. Here, a CMOS camera, a spectrometer, and an avalanche photodiode can be employed for diagnosis.

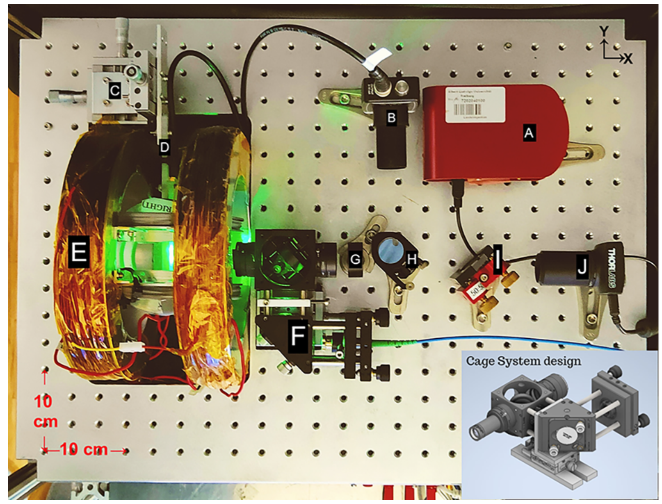

FIG. 6. Top view of a possible, final setup. Individual components are: (A) CCD spectrometer, (B) avalanche photo diode, (C) translation stage for microstrip on mount (D), (E) three coil pairs in (near) Helmholz configuration for magnetic field control – with large, medium, and small diameters – (F) cage system combining a fibre coupler, a mirror, a dichroic mirror, an aspheric 10-mm focal length lens, and a 125-mm focal length lens, (G) optical long pass filter, beam splitters 90:10 (H) and 50:50 (I), and (J) CMOS camera.

make use of chain of microwave components. The microwave signal is taken from the tracking generator of a spectrum analyser. In turn, the input of that same analyser can be employed to characterise all other microwave components. Note, the maximum input power of the spectrum analyser is 30 dBm, i.e., do not connect the output of the main amplifier to it! These components are, e.g., an input coupler, attenuators, and a high-power amplifier with an maximum output of 16 W. We designed and our electronics workshop manufactured a grounded coplanar waveguide where we can place the diamonds and send in the microwave signal for recording the magnetic resonances. Further, in each lab course students may decide to build a low-pass filter using their choice of resistors and capacitors to filter noise picked up by the APD signal. For amplifying the fluorescence signal recorded by the APD, we can use, e.g., an audio amplifier with variable gain. Alternatively, we can also use a photo multiplier tube (PMT) module to record fluorescence photons.

Keywords: oscilloscope, frequency generator, spectrum analyser, tracking generator, microwaves, grounded coplanar waveguide, directional coupler, attenuator, high/low-pass filter, power splitter, power detector, and decibel scale.

C. Apparatus for NV centre spectroscopy

One possible realisation of a final apparatus that needs to be set up by the students for the spectroscopy of individual diamonds is depicted in Fig. 5. It can be used for the measurements described in Sec. III C and can give results that are comparable to the descriptions in Sec. I C. It combines diamonds placed on the micro-strip PCB board that is fed by the amplified output of the tracking generator of the spectrum analyser. In this way, up to 42 dBm of microwave power in the range of $\omega_{\mathrm{mw}}/(2\pi) \simeq 2.0\,\mathrm{GHz}$ to $3.0\,\mathrm{GHz}$ can be applied for the measurements. Note, the temperature of the PCB board is monitored and when it's temperature reaches about 40 °C, the source needs to be turned off. Further, the laser beam is focused onto a specific diamond for characterisation and, ideally, to excite NV fluorescence. The fluorescence light is collected by the aspheric lens and guided toward the detection region, where it can be recorded by the CMOS camera, the spectrometer, and the APD. Corresponding signals can be monitored on the PC or the oscilloscope. Depending on the type of measurement, optical and electronic filters or amplifiers can be placed various positions. More, we tune the magnetic field strength and orientation on site of the diamonds using three field coil pairs with small (S), medium (M), and large (L) diameters in near Helmholz configuration. Table I lists relevant properties of the coil pairs and in Figure 6, we show a picture of a possible optical setup including the coils.

Prep. question example: "What are the main components of the experimental setup and what are they used for?"

TABLE I. Properties of magnetic field coil pairs.

Description	Inner / outer diameter (mm)	No. of windings	Field strength in centre per current (µT/A)
Large coil pair	141(1) / 213(1)	340(L1) and 360(L2)	3000.2(8)
Medium coil pair	128(1) / 102(1)	26(M1) and 22(M2)	316.5(2)
Small coil pair	96(1) / 70(1)	23(S1) and 26(S2)	450.3(2)

III. COURSE PROGRAM

A. Notes on performing measurements and data analysis

For a proper conduct and analysis of experiments it is vital to take corresponding (hand written) lab notes on stapled paper with page numbers. Notes need to include sketches of build setups used for each kind measurements, a description of experimental sequences, and a list of all experimental parameters (including uncertainties) and results. In case results are taken with a data acquisition systems corresponding files names are to be written down. To ensure that chosen experimental setups and results are reasonable, it is required to make a preliminary analysis of recordings, estimate uncertainties, and noted in the lab notes. A final analysis of results requires a more involved assessment of the data. In particular this includes appropriate model fits to the data to extract best values for measurement results and detailed quantification of systematic and statistical uncertainties.

At last a final report summarises the findings in a separate document that can stand on its own and can be comprehend by colleagues who did not participate in the work, see also the supplied checklist. This report includes, e.g., a short introduction into the topic and puts the conducted experiments into context, a descriptions of experimental setups, shows raw data, discusses the performed analysis, and gives final values with uncertainties. In the last section of the report, findings are summarised and discussed including an outline of short-comings of deployed measurements and future improvements. In any case, we strongly encourage students to discuss requirements with the assigned teaching assistant.

B. Calibration measurements

In order to investigate and judge systematic effects and corresponding uncertainties of main findings taken with an experimental apparatus, it is necessary to perform independent calibration measurements, analyse calibration results, and carefully consider those results in all further measurements. To ensure proper calibration it can even be necessary to perform such measurements multiple times, interleaving main experimental sequences. In addition, these calibrations are part of an optimisation of experimental parameters. In case of our lab course independent calibration measurements are, e.g., required for the:

- Laser wavelength, beam power, and waists,
- Optical spectrometer, filters, mirrors, and lenses,
- Camera (CMOS chip) image magnification and resolution,
- Collection efficiency of imaging setup and transmission for green and red light,
- Reflection, loss and transmission the micro-strip transmission line,
- Gain of the microwave amplifier, power fed into micro-strip
- Strength and orientations of external magnetic fields and stray fields.

Due to the limited duration of the lab course, students need to prioritise the calibrations and employ corresponding benchmark setups. In some cases, students may choose that manufacture specifications suffice for calibration. But in such cases, students need to include these calibrations and state their reasoning for doing so in the lab notes and/or the protocol. Based on any kind of calibration, students judge if accessible or chosen parameter regimes are reasonable adjusted/optimised for the intended purposes.

C. Compare the characteristics of multiple diamonds

The main objective of the lab course focuses on the characterisation and comparison of multiple micro-sized diamonds and their enclosed NV centres. Such comparison relies on the measurement of several figure of merits and students can replicate or build a variation of the apparatus described in Sec. II C for this investigation. In the following, we give a list of examples of these figure of merits:

- Size and shape of the diamonds,
- Fluorescence spectra,
- Microwave spectrum with approx. zero external magnetic field,

- Number of NV centre orientations within the monocrystal,
- Orientation of the diamond lattice in the laboratory frame.

Students choose appropriate measurement sequences after a discussions with the tutor to determine these values. Finally, they can record sequences with variable magnetic field strengths using their *favourite* diamond as a magnetic field probe and determine the corresponding magnetic field sensitivity.

IV. APPENDIX

In Table II, we list all available equipment and corresponding manuals are stored on the lab computer or can be found online (following the links).

[1] I. Aharonovich, A. D. Greentree, and S. Prawer, Nat. Photonics **5**, 397 (2011).
[2] T. D. Ladd, F. Jelezko, R. Laflamme, Y. Nakamura, C. Monroe, and J. L. O'Brien, Nature **464**, 45 (2010).
[3] V. N. Mochalin, O. Shenderova, D. Ho, and Y. Gogotsi, Nat. Nanotechnol. **7**, 11 (2011).
[4] I. Aharonovich, S. Castelletto, D. A. Simpson, C.-H. Su, A. D. Greentree, and S. Prawer, Reports Prog. Phys. **74**, 076501 (2011).
[5] M. W. Doherty, N. B. Manson, P. Delaney, F. Jelezko, J. Wrachtrup, and L. C. Hollenberg, Phys. Rep. **528**, 1 (2013).
[6] I. M. Georgescu, S. Ashhab, and F. Nori, Rev. Mod. Phys. **86**, 153 (2014).
[7] R. Schirhagl, K. Chang, M. Loretz, and C. L. Degen, Annu. Rev. Phys. Chem. **65**, 83 (2014).
[8] J. Wrachtrup, Ger. Res. **37**, 20 (2015).
[9] D. J. Wineland, Rev. Mod. Phys. **85**, 1103 (2013).
[10] D. Leibfried, R. Blatt, C. Monroe, and D. Wineland, Rev. Mod. Phys. **75**, 281 (2003).
[11] G. Balasubramanian, I. Y. Chan, R. Kolesov, M. Al-Hmoud, J. Tisler, C. Shin, C. Kim, A. Wojcik, P. R. Hemmer, A. Krueger, T. Hanke, A. Leitenstorfer, R. Bratschitsch, F. Jelezko, and J. Wrachtrup, Nature **455**, 648 (2008).
[12] J. R. Maze, P. L. Stanwix, J. S. Hodges, S. Hong, J. M. Taylor, P. Cappellaro, L. Jiang, M. V. G. Dutt, E. Togan, A. S. Zibrov, A. Yacoby, R. L. Walsworth, and M. D. Lukin, Nature **455**, 644 (2008).
[13] J. M. Taylor, P. Cappellaro, L. Childress, L. Jiang, D. Budker, P. R. Hemmer, A. Yacoby, R. Walsworth, and M. D. Lukin, Nat. Phys. **4**, 810 (2008).
[14] F. Dolde, H. Fedder, M. W. Doherty, T. Nöbauer, F. Rempp, G. Balasubramanian, T. Wolf, F. Reinhard, L. C. L. Hollenberg, F. Jelezko, and J. Wrachtrup, Nat. Phys. **7**, 459 (2011).
[15] D. M. Toyli, D. J. Christle, A. Alkauskas, B. B. Buckley, C. G. Van de Walle, and D. D. Awschalom, Phys. Rev. X **2**, 031001 (2012).
[16] M. W. Doherty, V. V. Struzhkin, D. A. Simpson, L. P. McGuinness, Y. Meng, A. Stacey, T. J. Karle, R. J. Hemley, N. B. Manson, L. C. Hollenberg, and S. Prawer, Phys. Rev. Lett. **112**, 047601 (2014).
[17] L. P. McGuinness, Y. Yan, A. Stacey, D. A. Simpson, L. T. Hall, D. Maclaurin, S. Prawer, P. Mulvaney, J. Wrachtrup, F. Caruso, R. E. Scholten, and L. C. L. Hollenberg, Nature Nanotechnology **6**, 358 (2011).
[18] O. Arcizet, V. Jacques, A. Siria, P. Poncharal, P. Vincent, and S. Seidelin, Nat. Phys. **7**, 879 (2011).
[19] P. Maletinsky, S. Hong, M. S. Grinolds, B. Hausmann, M. D. Lukin, R. L. Walsworth, M. Loncar, and A. Yacoby, Nat. Nanotechnol. **7**, 320 (2012).
[20] V. R. Horowitz, B. J. Alemán, D. J. Christle, A. N. Cleland, and D. D. Awschalom, Proc. Natl. Acad. Sci. **109**, 13493 (2012).
[21] O. M. Maragò, P. H. Jones, P. G. Gucciardi, G. Volpe, and A. C. Ferrari, Nat. Nanotechnol. **8**, 807 (2013).
[22] D. Palani, "Benchmarking micro-diamonds for sensing applications," (2019).
[23] L. M. Pham, *Magnetic field sensing with nitrogen-vacancy color centers in diamond*, Tech. Rep. (DTIC Document, 2013).

TABLE II. List of available equipment

Description	Vendor	Part No.	Specifications
Laser	Toptica	IBEAM-SMART-515-S	$< 100\,\mathrm{mW}$ at $\simeq 519\,\mathrm{nm}$
Compact CCD Spectrometers	Thorlabs	CCS175/M	see: link
CMOS Camera	Thorlabs	DCC1545M	see: link
Avalanche photo diode	Thorlabs	APD430A2/M	see: link
Spectrum analyser (with tracking generator)	RIGOL	DSA 1030	$<$ 10dBm form $9\,\mathrm{kHz}$ to $3.0\,\mathrm{GHz}$
Oscilloscope	RIGOL	DS1054Z	$\leq$ 50 MHz
Microwave amplifier	Mini Circuits	ZHL-16W-43-S+	see link
Audio amplifier			
Aspheric lens	Thorlabs		
Plano-convex lens	Thorlabs		
Dichroic Mirror	Thorlabs	DMLP550	
$2\times$ Optical longpass filter	Thorlabs	FELH0600	
Optical band-pass filter	Thorlabs		
Optical beam spliter 50:50	Thorlabs		
Optical beam spliter 90:10	Thorlabs		
Optical power meter	Thorlabs	PM160T	
Coupler for microwaves	Mini-Circuits	ZADC-10-63-S+	
Magnetic field sensor	PCE	PCE-MFM 3000	